Published in final edited form as:
J Biol Chem. 2007 May 25; 282(21): 15404–15415.

THROMBOSPONDIN-1 INHIBITS NITRIC OXIDE SIGNALING VIA CD36 BY INHIBITING MYRISTIC ACID UPTAKE*

Jeff S. Isenberg‡, **Yifeng Jia**‡, **Julia Fukuyama**‡, **Christopher H. Switzer**§, **David A. Wink**§, and **David D. Roberts**‡1

‡*Laboratory of Pathology, Center for Cancer Research, National Cancer Institute, National Institutes of Health, Bethesda, Maryland 20892*

§*Radiation Biology Branch, Center for Cancer Research, National Cancer Institute, National Institutes of Health, Bethesda, Maryland 20892*

Abstract

Although CD36 is generally recognized to be an inhibitory signaling receptor for thrombospondin-1 (TSP1), the molecular mechanism for transduction of this signal remains unclear. Based on evidence that myristic acid and TSP1 each modulate endothelial cell nitric oxide signaling in a CD36-dependent manner, we examined the ability of TSP1 to modulate the fatty acid translocase activity of CD36. TSP1 and a CD36 antibody that mimics the activity of TSP1 inhibited myristate uptake. Recombinant TSP1 type 1 repeats were weakly inhibitory, but an anti-angiogenic peptide derived from this domain potently inhibited myristate uptake. This peptide also inhibited membrane translocation of the myristoylated CD36 signaling target Fyn and activation of Src family kinases. Myristate uptake stimulated cGMP synthesis via endothelial nitric oxide synthase and soluble guanylyl cyclase. CD36 ligands blocked myristate-stimulated cGMP accumulation in proportion to their ability to inhibit myristate uptake. TSP1 also inhibited myristate-stimulated cGMP synthesis by engaging its receptor CD47. Myristate stimulated endothelial and vascular smooth muscle cell adhesion on type I collagen via the NO/cGMP pathway, and CD36 ligands that inhibit myristate uptake blocked this response. Therefore, the fatty acid translocase activity of CD36 elicits pro-angiogenic signaling in vascular cells, and TSP1 inhibits this response by simultaneously inhibiting fatty acid uptake via CD36 and downstream cGMP signaling via CD47.

Pathological angiogenesis or the lack thereof underlies a number of major diseases (1). Proangiogenic signals from vascular endothelial growth factors (VEGF[1]) and fibroblast growth factors (FGF1 and FGF2) to induce blood vessel formation are opposed by signals from endogenous angiogenesis inhibitors, including two thrombospondins (TSP1 and TSP2) and proteolytic fragments of several extracellular matrix components (2,3). Defining the mechanism of action of these inhibitors has been complicated by the finding that vascular cells express multiple receptors for several of these molecules. In the case of TSP1, endothelial cells express at least 8 receptors, and some of these elicit pro- rather than anti-angiogenic responses

*This research was supported by the Intramural Research Program of the NIH, National Cancer Institute, Center for Cancer Research.

1To whom correspondence should be addressed: NIH, Building 10, Room 2A33, 10 Center Dr MSC1500, Bethesda, MD 20892 phone (301)496-6264, e-mail: droberts@helix.nih.gov.

[1]The abbreviations used are: cGK, cGMP-dependent protein kinase; EGM, endothelial growth medium (with additives); EBM, endothelial basal medium (without additives); eNOS, endothelial nitric oxide synthase; FAF, fatty acid free; FGF, fibroblast growth factor; HAVSMC, human aortic vascular smooth muscle cells; HUVEC, human umbilical vein endothelial cells; L-NAME, N-nitro-L-arginine methyl ester; MetAP2, methionine aminopeptidase-2; ODQ, 1H-[1,2,4]oxadiazole[4,3-a]quinoxalin-1-one; Rp-8-*p*CPT-cGMPs, 8-(4-chlorophenylthio)guanosine- 3′,5′-cyclic monophosphorothioate, Rp-isomer; sGC, soluble guanylyl cyclase; SM-BM, smooth muscle cell basal medium; SM-GM, smooth muscle cell growth medium; SSO, sulfosuccinimidyl oleate; TSP1, thrombospondin-1; TSR, TSP1 type 1 repeats; VEGF, vascular endothelial growth factor; VSMC, vascular smooth muscle cells

(4,5). The activities of some TSP1 receptors differ between large vessel and microvascular endothelial cells, and some are regulated by specific contextual signals (4–6).

CD36, a member of the scavenger receptor B family, is a TSP1 receptor that is selectively expressed in microvascular endothelium (7,8). CD36 was initially reported to recognize CSVTCG sequences in the type 1 repeats of TSP1(9), but further studies identified higher affinity binding to the adjacent GVQXR sequences in the second and third type 1 repeats (10,11). CD36 binding was markedly enhanced by epimerization of the first Ile in a peptide from the second type 1 repeat ^{434}GDGV($_{D}$-I)TRIR^{442} (11). TSP1, recombinant type 1 repeats of TSP1, and peptide mimetics of its CD36-binding sequences inhibit FGF2-stimulated endothelial cell migration and induce apoptosis *in vitro* and inhibit FGF2-induced corneal angiogenesis *in vivo.* The proapoptotic signal from CD36 requires activation of the Src family kinase p59-Fyn, signaling through p38, and downstream activation of caspase-3-like proteases (12). JNK-1 is also involved in the anti-motility activity of TSP1 mediated by CD36 (13). Combined with the observation that several Src family kinases co-immunoprecipitate with CD36 (14,15), these results imply that TSP1 signals through CD36 via a physical coupling to Fyn activation. However, a subsequent study concluded that Src kinases and CD36 mutually associate with lipid rafts but lack any direct binding interaction (16).

We recently identified a new downstream target for the anti-angiogenic activity of TSP1 that involves CD36 (17). Low concentrations of nitric oxide (NO) stimulate angiogenesis through a cGMP-dependent pathway. NO is synthesized in endothelial cells by endothelial nitric oxide synthase (eNOS), and eNOS in turn is activated by Akt-mediated phosphorylation of eNOS stimulated by VEGF signaling (18). Several studies have provided evidence that NO is an essential mediator of VEGF-stimulated angiogenesis (19,20). We found that NO-stimulated cGMP signaling in both endothelial and vascular smooth muscle cells is potently inhibited by picomolar concentrations of TSP1, its type 1 repeats, and CD36 antibodies (17,21) In endothelial cells, TSP1 blocked VEGF-stimulated cGMP synthesis.

Although engaging CD36 is sufficient to inhibit NO signaling as well as VEGF-induced cGMP formation, we subsequently found that CD36 is not necessary for the same activity of intact TSP1 (21,22). Rather, we found that the TSP1 receptor CD47 is necessary and sufficient for the anti-angiogenic signal elicited by picomolar concentrations of TSP1. However, a weaker inhibitory activity of TSP1, observed at 1–10 nM, was deficient in CD36 null vascular cells (22). Furthermore, synthetic derivatives of CD36-binding peptides, similar to those currently in phase II clinical trials as angiogenesis inhibitors (23,24), required CD36 for their ability to potently inhibit NO signaling. It is important, therefore, to identify the molecular mechanism by which TSP1, these TSP1 mimetics, and CD36 influence NO signaling in endothelial and vascular smooth muscle cells.

CD36 also has fatty acid translocase activity (reviewed in (25)). Myristic acid was recently shown, in a CD36- and AMP kinase-dependent manner, to activate eNOS (26). This observation prompted us to ask whether TSP1 and its CD36 binding sequences might modulate NO signaling through antagonizing fatty acid uptake via CD36 and thereby inhibit endogenous NO synthesis. We report here that TSP1 inhibits both signaling and functional responses of endothelial cells elicited by myristate. Although myristate uptake into some cells may not require CD36 and the activity of myristate to activate eNOS was inferred on this basis to be independent of uptake (26), we now show that TSP1 peptide mimetics are potent inhibitors of myristate uptake into endothelial cells. Consistent with its known effect on eNOS activity (26), myristate treatment of endothelial cells elicits similar functional and biochemical responses as exposure to an NO donor, and these responses are effectively blocked by TSP1 peptide mimetics and other CD36 ligands that inhibit its translocase activity. We further show

that membrane targeting of the known CD36 signaling target Fyn is stimulated by myristate and inhibited by antagonist ligands.

EXPERIMENTAL PROCEDURES

Cells and Reagents

HUVEC and HAVSMC (Cambrex, Walkersville, MD) were maintained in either endothelial cell growth medium (EGM, Cambrex) with 2% FCS or vascular smooth muscle growth medium (SMGM, Cambrex) with 2% FCS in 5% CO_2 at 37° C. Cells were utilized at passages 4–8. CD47 null VSMC were prepared from aortic segments from knock out mice and grown in vascular smooth muscle growth medium as described (22). Cells were used between passages 2 through 8. TSP1 was prepared from human platelets obtained from the Blood Bank of the Clinical Center of the NIH as previously described (27). The recombinant fragment of the type I repeat domain of TPS1 (3TSR) was graciously provide by Dr. Jack Lawler (Harvard University). TSP1-derived peptides ^{488}VTAGGGVQKRSRL^{500} (p906) and ^{434}GDGVDITRIR^{442} (p907) were synthesized by Peptides International (Louisville, KY). The underlined residues indicate modifications from the natural TSP1 sequence. Additional CD36-(^{488}VTCGGGVQKRSRL^{900}, p245) and CD47-binding peptides (^{1102}FIRVVMYEGKK^{1112}, p7N3) derived from TSP1 were available from previous studies. The CD36 antagonist antibody clone FA6-152 was obtained from Immunotech (Beckman Coulter, Fullerton, CA). The CD36 agonist antibody clone SMΦ was purchased from Chemicon International (Temecula, CA). 1H-[1,2,4]Oxadiazole[4,3-a]quinoxalin-1-one (ODQ), N-nitro-L-arginine methyl ester (L-NAME), fatty acid free bovine serum albumin (FAF-BSA), myristic acid, and oleic acid were obtained from Sigma-Aldrich. [^{3}H]-myristic acid was also obtained from Sigma. Type I bovine dermal collagen was obtained from Inamed Biomaterials (Santa Barbara, CA). Human vitronectin was obtained from Sigma. Fibronectin was purified from human plasma (28), and a 33 kDa recombinant fragment containing the α5β1 integrin binding site of fibronectin (FN-33) was provided by Dr. Tikva Vogel (29). cGMP measurement was performed with an immunoassay kit obtained from Amersham Bioscience (Piscataway, New Jersey). The PKG inhibitor Rp-8-*p*CPT-cGMPs was obtained from Calbiochem (EMD Biosciences, San Diego, CA). A CD36 morpholino phosphorodiamidate oligonucleotide targeting the human protein and having the sequence GCCCACAGTTCCGGTCAAGCCCAT was purchased from Gene Tools (Philmoth, OR) along with a 5 base mismatched control morpholino (GCgCAgAGGTTCCGcTCACAcCCgAT).

Immunoprecipitation of CD36

HUVEC and HAVSMC were cultured in standard growth medium on 10 cm^2 culture plates to a density of 90% surface saturation and harvested with EDTA. Cell pellets were washed 3× with cold DPBS and cells counted. Equal cell numbers were incubated with Sulfo-NHS-LC-Biotin (Pierce, Rockford, IL) (1 mg/100 μl molecular grade water) for 30 min at room temperature and washed again 3× in cold DPBS. The cell pellet was resuspended in RIPA buffer containing 1mM PMSF, incubated for 20 minutes at 4° C and centrifuged at 13000 rpm for 15 min. The supernatant was incubated with protein G ferrous beads (Dynabeads, Dynal Biotech, Olso, Norway) and a monoclonal CD36 antibody, clone FA6-152 (Immunotech, Beckman Colter) over night at 4 °C. Beads were washed with cold RIPA buffer 3× and then boiled in sample buffer at 95 °C for 10 min. Protein levels of samples were then determined by MicroBCA assay (Pierce, Rockford, IL), and equal amounts of protein loaded and electrophoresed in 4–12% BisTris NuPAGE gels and transferred to PVDF membranes. Membranes were blocked with PBS and 3% BSA for 1 hr, incubated with streptavidin (1:20,000) (Sigma, St. Louis, MO) for 1 hr, and then developed with Visualizer Spay & Glow (Upstate, lake Placid, NY).

CD36 knockdown experiments

HUVEC were treated as per the manufacturer's recommendations in growth medium with the indicated concentrations of CD36 antisense or mismatched control morpholino for 48 h prior to analysis.

Sulfosuccinimidyl oleate (SSO) Synthesis

SSO was synthesized as described (30). Briefly, 0.25 mmoles each of oleic acid and N-hydroxysulfosuccinimide and 0.275 mmoles of dicyclohexylcarbodiimide were reacted in 0.5 ml anhydrous N,N-dimethylformamide overnight at room temperature. The dicyclohexylurea was crystallized out, and the solution filtered, and chilled. The product was then precipitated out of solution by the addition of cold ethyl acetate and dried under vacuum over phosphorous pentoxide. Working solutions of SSO were prepared immediately prior to each use.

Cell Adhesion

Cell adhesion was carried out in 96-well plates (Nunc, Denmark). After precoating wells with type I collagen (3 μg/ml), vitronectin (1 or 2 μg/ml), fibronectin (3 μg/ml), or FN-33 (1.5 or 3 μg/ml) HUVEC, HAVSMC or CD47 null VSMC were plated at a density of 1×10^4 cells/well in EBM or SM-BM containing 0.1% FAF-BSA and treatment agents and incubated in 5% CO_2 for 1 h. Wells were washed with PBS, and the cells were fixed with 1% glutaraldehyde for 10 min., washed and stained with 1% crystal violet for 20 min. Excess stain was rinsed away, the cells were extracted with 10% acetic acid, and the plates read at 570 nm.

Intracellular cGMP Measurement

HUVEC or HAVSMC were plated in 96-well culture plates at a density of 5×10^3 cells/well in EGM or SM-GM + 2% FCS. Following 24 h incubation, cells were weaned to EBM or SM-BM + 1% FCS and incubated an additional 24 h. Cells were then treated in EBM or SM-BM + 0.1% FAF-BSA with myristic acid at the indicated concentrations. Following a 5 min incubation, cells were lysed and intracellular cGMP determined by immunoassay ELISA as per the manufacturer's instructions.

[^{3}H]-Myristic Acid Uptake

The [^{3}H]-myristic acid uptake assays were performed using 80–90% confluent HUVEC cells (5×10^5 cells/well) in 24-well culture plates (Nunc, Denmark). Trace amounts of [^{3}H]-myristic acid (5 μCi/ml, 0.9 μM) mixed with 9.1 μM nonradioactive myristic acid were dissolved in a FAF-BSA solution at a myristic acid/BSA molar ratio of 1:2. Cells were incubated in medium with treatment agents for the indicated time intervals at 37°C. The uptake was stopped by removal of the solution followed by the addition of chilled 0.9% NaCl with 0.5% BSA. The stop solution was discharged, and the cells were washed again with stop solution. Cell were lysed by adding 0.2 M NaOH (200 μl/well) and incubating for 2 h at 37° C. On completion of solubilization, 0.2 M HCl in 1.5 M Tris-HCl (200 μl) was added to each well. Radioactivity was determined in 10 ml of Ecoscint A (National Diagnostics, Atlanta, GA) using a 1900CA liquid scintillation counter (Packard).

Detection of Fyn translocation

HUVEC were plated on 100 mm plates in 2 %FCS EGM and grown to 80% confluence. Cells were weaned over 24 h to EBM containing 1% FCS. Following weaning, cells were pre-treated in EBM containing 0.1% FAF-BSA ± peptide p907 (10 μM) for 15 min, then incubated for 1 h in the presence of myristate (10 μM). Following treatment, cells were rinsed, scraped in ice-cold STE (50 mM Tris-HCl, pH 7.4, 150 mM NaCl, and 1 mM EDTA, 1× protease inhibitor cocktail tablet (Roche)) and centrifuged at 1500 rpm for 5 min. The cell pellet was resuspended

into 200 μl of hypotonic buffer (10 mM Tris-HCl, pH 7.2, 0.2 mM $MgCl_2$, 100 mM Na_3VO_4, and 1× protease inhibitor cocktail tablet) and homogenize with 30 strokes in a 1.5 ml Dounce homogenizer. To insure a complete cell lysis, cells were freeze-thawed twice at −80 °C. The homogenate volume was adjusted to a final concentration of 250 mM sucrose and 1 mM EDTA and centrifuged for 45 min at 100,000 xg. The S100 fraction was collected into 4× SDS sample buffer, and P100 was collected into 1× SDS sample buffer. Samples were separated by electrophoresis and blotted onto PVDF. Membranes were probed with anti-Fyn Ab (BD Transduction Laboratories, Cat: 610163) or eNOS (BD Transduction Laboratories) at 4 °C overnight and followed by an hour incubation at RT with goat-anti-mouse secondary antibody conjugated with horseradish peroxidase (Jackson ImmunoResearch). After washing with TBS, the bound antibodies were detected by ECL (Pierce). The membrane was then reprobed with anti-actin antibody (Sigma) for loading control.

Detection of Src family kinase phosphorylation

HUVEC were starved overnight in EBM containing 1% FCS, rinsed and treated with the indicated reagents in EBM with 0.1% FAF-BSA. Cells were treated with p907 (10 μM) for 15 min before the addition of VEGF or myristate. VEGF was added at 20 ng/ml for 5 minutes and myristate (10 μM) for 15 min. Cells were then rinsed with PBS and collected in SDS sample buffer, separated by electrophoresis and blotted onto PVDF membranes. Membranes were probed with anti-Src-Y416 Ab (Cell Signaling) or anti-Src Ab (Cell Signaling). Membranes were reprobed with anti-actin antibody for loading control.

Statistics

All assays were repeated at least in triplicate and are presented as the mean ± SD with significance being determined by the Students t test for a $p > 0.05$.

RESULTS

Inhibition of myristic acid uptake by TSP1, CD36-binding peptides, and SSO

To assess the ability of TSP1 to modulate the fatty acid translocase activity of CD36, HUVEC at approximately 80% confluence were transferred into serum-free medium and treated with [^{3}H]-myristic acid (10 μM) pre-complexed with 0.1% FAF BSA. Myristic acid uptake under these conditions was time dependent, and 5 min was used for subsequent experiments (Fig. 1A). Preincubation of HUVEC with exogenous TSP1 before incubating for 5 min with [^{3}H]-myristic acid at 37 °C dose dependently inhibited up to 60% of myristic acid uptake (Fig 1B). Recombinant type 1 repeats of TSP1 (3TSR) were less effective, reaching significance only at 483 nM, whereas the CD47-binding CBD of TSP1 did not significantly inhibit myristic acid uptake (Fig. 1B). This inhibitory activity was specific for TSP1 in that equimolar concentrations of laminin-1 and vitronectin were inactive. Myristate uptake into human aortic VSMC was also inhibited in a dose dependent manner by TSP1 (Fig. 1C).

Myristate uptake in HUVEC was not significantly inhibited by a reported CD36-binding peptide from the third type 1 repeat of TSP1 (p245, VTCGGGVQKRSRL) or a derivative of the same peptide in which the native Cys was substituted with Ala to prevent dimerization (p906, VTAGGGVQKRSRL, Fig. 1D). However, uptake of myristic acid was strongly inhibited in the presence of ≥0.1 μM of the CD36-binding peptide GDGV$_D$ITRIR derived from the second type 1 repeat of TSP1 by epimerization of Ile^{438} to the D-isomer (11) (p907, Fig. 1D). As a further control, a CD47 binding peptide derived from the CBD of TSP1 also failed to inhibit myristate uptake (Fig. 1E).

To further examine the role of CD36 in myristate uptake into HUVECs, we tested the widely used antagonist of CD36 fatty acid translocase activity SSO (30,31). SSO dose dependently

inhibited up to 80% of [^{3}H]-myristic acid uptake in HUVEC, but its IC_{50} was approximately 100-fold higher than for the TSP1-based CD36 ligand p907 (Fig. 1F).

We confirmed CD36 expression in both vascular cell types by western blotting (Fig. 2A). Because expression was substantially higher in HAVSMC than in HUVEC, we used the former cells to confirm the role of CD36 in myristate uptake by knocking down CD36 expression using a translation blocking antisense morpholino oligonucleotide. Western blotting confirmed efficient suppression of CD36 protein expression at 10 μM of the morpholino (Fig. 2B), and this concentration decreased myristate uptake by approximately 50% (Fig. 2C). Activity of the antisense morpholino was specific in that a 5 base mismatched morpholino did not inhibit myristate uptake. The incomplete inhibition of myristate uptake by CD36 knock down is consistent with previous evidence for both CD36-dependent and CD36-independent uptake of free fatty acids into cells (32–34).

Myristic acid uptake is blocked by CD36 “agonist” but not by “antagonist” antibodies

The ability of different CD36 antibodies to mimic or block the anti-angiogenic activities of TSP1 and its derived peptides was presented as evidence that CD36 mediated this activity of TSP1 (10). CD36 antibody SMΦ, which is defined as an agonist because it replicates the activity of TSP1 as an angiogenesis inhibitor (10), potently inhibited myristic acid uptake into HUVEC at 10 ng/ml (Fig. 2D). In contrast, CD36 antibody FA6-152, which antagonized TSP1 in the same angiogenesis assays but did not itself inhibit angiogenic responses (10,12,13), had no effect upon myristic acid uptake into endothelial cells even at 10 μg/ml (Fig. 2D).

Thus, the CD36-dependent anti-angiogenic activities of TSP1, a peptide mimic of its type 1 repeats, and two CD36 antibodies correlate with their ability to inhibit the fatty acid translocase activity of CD36. Since CD36 has been implicated in the ability of exogenous myristic acid to activate eNOS (26) and in the ability of TSP1 to inhibit NO signaling in endothelial and VSMC (17,21), we considered that both vascular cell responses may be mediated by myristic acid transport via CD36, which provides a required precursor for myristoylation of more than 100 proteins, including several key signaling molecules (35).

One myristoylated protein that was shown previously to be a target of CD36 signaling in endothelial cells is the Src kinase Fyn (12). Myristoylation of Fyn is required for subsequent palmitoylation, methylation, membrane translocation, and some functional responses mediated by Fyn (36). Medium containing serum provided adequate myristic acid to maintain full Fyn association with the membrane (P100) fraction in HUVEC (Fig. 3A). In serum free medium, however, Fyn was localized primarily to the cytosolic (S100) fraction (Fig. 3A and results not shown). Under these conditions, translocation of Fyn from the cytosol to the cell membrane in HUVEC was rapidly stimulated by addition of 10 μM of myristic acid to the medium complexed with FAF BSA. The myristic acid-stimulated translocation, however, was prevented in the presence of p907 (Fig. 3A).

This translocation appears to increase Fyn activation because treatment of HUVEC in FAF BSA with myristate increased Tyr^{416} phosphorylation to a similar extent as the known Fyn activator VEGF (Fig. 3B) (37,38). Furthermore, addition of p907 strongly inhibited Tyr^{416} phosphorylation induced by myristate and to a lesser extent Tyr^{416} phosphorylation induced by VEGF (Fig. 3B). It should be noted that the Tyr^{416} antibody used is pan-Src reactive and two phosphorylated bands were apparent in most experiments, so other members of the Src family may also be activated in response to exogenous myristate in a CD36-dependent manner.

We also considered whether the reported CD36-dependent positive effect of exogenous myristate on eNOS activity (26) could result from regulating membrane translocation of this myristoylated enzyme (39,40). In contrast to Fyn, almost all eNOS was associated with the

membrane fraction in cells starved overnight regardless of treatment (Fig. 3A). The small amount of eNOS in the cytoplasmic fraction could be decreased by adding serum or myristate, but adding p907 only minimally increased the fraction of soluble eNOS. Therefore, the effects of myristate and p907 on NOS activity (see below) probably can not be explained by altered translocation of eNOS within the time scale of these experiments. However, the relative insensitivity of eNOS to myristate starvation for this time period is consistent with its slow turnover rate (41).

Myristic acid increases cGMP levels in endothelial cells via CD36 and is NOS-dependent

If myristate levels are rate limiting for the targeting or activity of signaling molecules that regulate the NO/cGMP pathway, such signaling should be stimulated by providing exogenous myristic acid, and agents that block myristic acid uptake through CD36 should inhibit this signaling. The low levels of NO produced by eNOS can not be directly measured, but soluble guanylyl cyclase (sGC) activation is a sensitive indicator of endogenous NO and can be assessed by intracellular cGMP formation (42). Treatment with myristic acid increased intracellular cGMP in HUVEC measured at 5 min in a dose dependent manner, with a maximum response occurring at a dose of 10 μM (Fig. 4A). Time course studies confirmed that the stimulatory effect of 10 μM myristic acid was rapid and transient, with maximal accumulation occurring at 5–10 min. (Fig. 4B and results not shown). Exogenous TSP1 at a concentration adequate to inhibit NO-stimulated cGMP accumulation (17) also inhibited myristic acid stimulated cGMP in HUVEC (Fig. 4C).

The myristate-stimulated accumulation of cGMP in HUVEC requires CD36 because pretreatment with the CD36 antisense morpholino but not a control morpholino decreased intracellular cGMP to basal levels (Fig. 4D). Similar results were obtained following CD36 knockdown in HAVSMC (Fig. 4E). To further confirm the CD36 translocase-dependence for myristic acid stimulated cGMP accumulation, we used the inhibitor SSO (Fig. 4F). No stimulation of cGMP accumulation by myristic acid was seen following preincubation of HUVEC with this translocase inhibitor.

Consistent with the CD36-dependent activation of eNOS by myristate (26), pretreatment of endothelial cells with L-NAME (500 μM) completely abrogated myristic acid stimulated cGMP (Fig. 4G), indicating that NOS activity is required for this cGMP response.

The potent CD36-binding peptide p907 at 10 μM completely inhibited myristic acid-stimulated intracellular cGMP (Fig. 5A), but the control p906 was inactive (Fig. 5B). These results are consistent with the differential activities of these two peptides to block the fatty acid transport activity of CD36 (Fig. 1).

Myristic acid stimulates endothelial cell adhesion via CD36

We previously reported that NO/cGMP signaling stimulates endothelial cell adhesion on type I collagen (17). Similarly, HUVEC cell adhesion on a type I collagen substrate was stimulated in a dose dependent manner by myristic acid and was optimal at 10 μM (Fig 6A), consistent with the optimal dose for cGMP accumulation (Fig. 4A). The effect of myristate on cell adhesion was specific in that similar concentrations of oleic acid were inactive, although oleic acid above 100 μM moderately increased cell attachment (Fig 6A).

To determine whether the effect of myristate on adhesion is substrate-dependent, we examined several proteins that mediate adhesion via different integrins (Fig. 6B). Myristate (10 μM) significantly enhanced HUVEC adhesion on fibronectin, a recombinant fragment of fibronectin containing its $\alpha_5\beta_1$ binding RGD sequence, and the $\alpha_v\beta_3$ ligand vitronectin as well as on the $\alpha_1\beta_1/\alpha_2\beta_1$ substrate type I collagen. Therefore, stimulation of endothelial cell adhesion by

myristate can be mediated by several integrins. As shown below, this property also generalizes to VSMC.

If myristic acid uptake via CD36 is responsible for the increase in HUVEC adhesion, then blocking the fatty acid translocase activity of CD36 using SSO (30,31) should also inhibit this response. Myristic acid-stimulated HUVEC adhesion to type I collagen was inhibited in a dose-dependent manner by SSO (Fig. 6C). Similarly, myristate-stimulated adhesion was abolished in cells pretreated with the CD36 antisense morpholino but not in cells pretreated with the mismatched control (Fig. 6D).

Myristate stimulates adhesion via the eNOS/sGC/cGK pathway

Stimulation of HUVEC adhesion by myristate required NOS activity based on inhibition of myristic acid stimulated cell adhesion by L-NAME (Fig. 6E). The primary target the low NO flux produced by eNOS is the regulatory heme in sGC. The role of sGC was confirmed by abrogation of myristate-stimulated cell adhesion in the presence of 10 μM ODQ (Fig. 6F). cGMP produced by sGC in turn regulates downstream signaling by activating cGK or cGMP-dependent ion channels. The specific cGK inhibitor Rp-8-*p*CPT-cGMPs inhibited adhesion stimulated by either myristate or nitric oxide (Fig. 6G), suggesting that cGK is the relevant target of cGMP for regulating adhesion in these cells.

TSP1 and other inhibitory CD36 ligands block myristate-stimulated cell adhesion

Exogenous TSP1 dose-dependently inhibited myristate-stimulated HUVEC adhesion on type I collagen (Fig. 7A). TSP1 at 2.2 nM similarly inhibited HAVSMC adhesion on type I collagen and on the $\alpha_5\beta_1$ binding domain of fibronectin but did not achieve significance in three independent experiments for myristate-stimulated adhesion on the $\alpha_v\beta_3$ substrate vitronectin (Fig. 7B and results not shown). Although TSP1 is a ligand for some of these integrins (43, 44), the binding affinities are too low for direct competition by 2.2 nM TSP1 to account for the observed inhibition.

The CD36-binding recombinant TSP1 type 1 repeats (3TSR) inhibited HUVEC adhesion to collagen driven by myristic acid at relatively high doses (Fig. 7C), consistent with its weak activity to inhibit myristic acid uptake (Fig. 1B), but myristate-stimulated adhesion was more sensitive to inhibition by the CD36-binding p907 (Fig. 7D). Consistent with their inability to significantly inhibit myristic acid uptake at achievable concentrations (Fig. 1C), two CD36-binding peptides lacking the D-Ile inversion, p906 and p245 (10,45), did not inhibit cell adhesion (Fig 7D, E). The activities of CD36 antibodies SMΦ and FA6 152 also paralleled their activity to inhibit myristic acid uptake (Fig. 2D). Ligation with the agonist CD36 antibody SMΦ dose-dependently inhibited myristic acid stimulated HUVEC adhesion (Fig. 7F), but the antagonist CD36 antibody FA6 152 did not (Fig. 7G).

CD47 ligation indirectly inhibits myristate signaling via CD36

Although the CD47-binding peptide 7N3 did not inhibit myristate uptake (Fig. 1E), it did inhibit myristate-stimulated cell adhesion (Fig. 8A). This could be explained by the ability of CD47 signaling to inhibit NO signaling in vascular cells at the level of sGC (22). In this case, some of the inhibition of myristate signaling by TSP1 seen in Fig. 7A could also be indirect and mediated by TSP1 binding to CD47. To test this hypothesis, we first compared the effect of myristate on adhesion of VSMC isolated from WT and CD47 null mice (Fig. 8B). Stimulation of adhesion by myristate was unaffected in a CD47 null background, indicating that CD47 is not necessary for signaling induced by myristate.

As seen for HUVEC, TSP1 (at a dose sufficient to elicit CD47 signaling but not sufficient to directly inhibit myristate uptake via CD36) significantly inhibited adhesion on collagen

stimulated by myristate of murine WT but not CD47 null VSMC (Fig. 8C). Therefore, TSP1 via CD47 can indirectly inhibit myristate signaling at the level of sGC.

DISCUSSION

Our data reveals that anti-angiogenic signaling initiated by the interaction of TSP1 and related ligands with CD36 results at least in part from inhibition of its fatty acid translocase activity. Those CD36 ligands that exhibit anti-angiogenic activity inhibit myristate uptake and myristate-dependent NO signaling and downstream cGMP-mediated effects on endothelial cell adhesion (Fig. 9). TSP1 is less potent for inhibiting fatty acid uptake than for inhibiting cGMP signaling via CD47, but this is consistent with the differential responses of murine CD36 null and wild type vascular cells to TSP1 (22). CD47-dependent anti-angiogenic signaling in the context of NO stimulation requires only picomolar concentrations of TSP1. Engaging CD47 does not inhibit myristate uptake but can inhibit myristate signaling downstream of NOS. An anti-angiogenic peptide derived from the CD36-binding type 1 repeats of TSP1, however, is a potent antagonist of fatty acid transport via CD36. This peptide inhibits NO/cGMP/cGK signaling in a NOS-dependent manner and so acts upstream of sGC, which is the major apparent target of CD47-mediated inhibition by native TSP1 (22). Therefore, TSP1 can inhibit two different steps in NO signaling by engaging CD36 versus CD47 on endothelial cells.

Our data suggest an alternate mechanism for the recently described connection between endogenous nitric oxide production and CD36 (26). Zhu and coworkers inferred that activation of NOS is mediated by binding of myristic acid and, to a lesser extent, palmitic acid to CD36 without internalization. We now show that agents that inhibit myristate uptake via CD36 prevent NOS-dependent cGMP synthesis. Therefore, uptake of myristate is probably involved in the previously reported NOS activation by this fatty acid. These new results also suggest a mechanistic basis for our previous observations that CD36 ligation modulates several NO-stimulated vascular cell responses (17,21). In support of this hypothesis, we found that basal HUVEC adhesion to collagen in growth medium containing only FAF BSA is significantly increased upon addition of myristate. Involvement of NO signaling in stimulation of endothelial cell adhesion by myristate was confirmed by its inhibition in the presence of the nonselective NOS inhibitor L-NAME, the sGC inhibitor ODQ, and the cGK inhibitor Rp-8-*p*CPT-cGMPs. Taken together these results suggest that the stimulatory effects of myristate on endothelial cell adhesion to type I collagen requires the generation of endogenous NO, which in turn activates sGC and leads to cGK activation via cGMP (Fig. 9).

In addition to regulating NO signaling, myristic acid modifies the function of a number of proteins via N-myristoylation (35), and exogenous myristate has been documented to be efficiently utilized for protein acylation by other cell types (46). One myristoylated protein that was previously implicated in TSP signaling via CD36 is Fyn (12). Although Fyn is necessary for induction of apoptosis and inhibition of corneal angiogenesis by TSP1 (12), other investigators have concluded that Fyn mediates pro-angiogenic signaling. Fyn is not required for the vascular permeability activity of VEGF (47) but is required for stimulation of mitogenesis and tube formation by VEGF (48). Fyn also contributes to endothelial tube formation and migration stimulated by FGF2 and angiopoietin-2 (49,50). Conversely, the angiogenesis inhibitor pigment epithelium-derived growth factor specifically down regulated FGF2-stimulated Fyn activity via Fes (50).

We now show that the positive effects of myristate on endothelial cell signaling and function are associated with increased membrane translocation of Fyn and functional activation of Src family kinases as assessed by Tyr^{416} phosphorylation. The rapid increase in Fyn translocation following addition of exogenous myristate that we observed is consistent with the previously reported rapid translocation of this Src kinase following myristoylation (51). Src localization

and activation may also be regulated via CD36-mediated myristate uptake because, unlike Fyn, Src is exclusively tethered to membrane via myristoylation (52).

Fyn and other Src family kinases are known to co-precipitate with CD36 in lysates from platelets and endothelial cells (14,15), but given their mutual association with lipid raft microdomains this is not proof of their direct interaction. Indeed, a more detailed examination failed to detect direct interaction of Fyn with CD36 (16). Our results show that independent of any potential physical coupling, the fatty acid translocase activity of CD36 can modulate Fyn function by altering its cellular localization and functional activation. Therefore, regulation of Fyn by CD36 probably does not require any physical interaction.

It was surprising that exogenous myristic acid would be required for protein myristoylation given that myristic acid is an abundant component of cellular phospholipids. Presumably, the free fatty acid pool must be limiting for synthesis of myristoyl-CoA in HUVEC deprived of serum. Additional studies are required to determine whether CD36 globally limits protein myristoylation or acts specifically to regulate trafficking of certain targets such as Fyn. We previously found that TSP1 also inhibits signaling downstream of cGMP (17). Inhibiting myristoylation was previously shown to prevent membrane localization of cGMP-dependent protein kinase II (53). This, therefore, is a potential target for the latter activity of TSP1.

The results of Zhu (26) and our results, showing L-NAME inhibition of myristate-induced cGMP signaling, indicate that exposure of serum-deprived HUVEC to exogenous myristate rapidly activates eNOS. This could occur by regulation of eNOS myristoylation, which is essential for its membrane localization and function (39,40,54) However, the efficient cotranslational myristoylation of eNOS coupled with further palmitoylation may make this target less sensitive to limiting the myristic acid pool (41). Furthermore, the ~20 h half life of eNOS may preclude detecting a significant shift in distribution of eNOS within the 1 h period of our assay. Because the activity of eNOS is regulated by exogenous myristate within this time frame, translocation of other myristoylated proteins that control eNOS activation, such as the phosphatase PP2B and certain myristoylated peptides (55–57) should be considered. Future studies will examine which myristoylated proteins are responsive to CD36-mediated myristate uptake within the time frame of eNOS activation.

Our observations that CD36 limits myristate uptake and the myristate/CD36-dependent translocation of at least one important signaling protein suggest a common basis for the activities of CD36- and methionine aminopeptidase (MetAP2)-targeted drugs as angiogenesis inhibitors (Fig. 9). MetAP2 inhibitors such as fumagillin, ovalicin, and TNP-470 prevent cleavage of the N-terminal Met from proteins destined to be myristoylated (58). CD36 transports myristic acid that can be activated by acyl-CoA synthetases to become the substrate for N-myristoyl transferases. Although myristic acid is abundant in membrane phospholipids, our data and that of Zhu (26) indicates that the availability of free myristic acid is limiting for regulation of eNOS in serum starved endothelial cells.

This common mechanism is relevant to development of therapeutic angiogenesis inhibitors. Irreversible MetAP2 inhibitors such as TNP470 have toxic side effects that have prompted efforts to develop reversible inhibitors of MetAP2 (59). Our data suggests that the CD36-directed drug ABT-510 may show better efficacy by reversibly blocking access to the myristoyl-CoA needed for tethering Fyn and other signaling proteins to membranes subsequent to MetAP2 cleavage of the terminal Met.

TNP-470 shares with ABT-510 the property of synergizing with radiation to inhibit tumor angiogenesis (60–62). Similar synergism with cytotoxic agents was also noted for TNP-470 and ABT-510 (63,64). The convergent effects of these two drugs on protein myristoylation may explain these similarities. Furthermore, the myristoylation pathway may play a more

general role in tumor growth independent of angiogenesis. N-myristoyl transferases have been considered as potential targets for anti-neoplastic drugs (65), and MetAP2 is elevated in colon carcinoma (66). Therefore, drugs that target CD36, such as ABT-510, may also have anti-tumor activities through inhibiting myristate uptake that are independent of angiogenesis.

Acknowledgments

We thank Drs. Jack Lawler and Bill Frazier for providing reagents.

References

1. Carmeliet P. Nature 2005;438(7070):932–936. [PubMed: 16355210]
2. Lawler J, Detmar M. Int J Biochem Cell Biol 2004;36(6):1038–1045. [PubMed: 15094119]
3. Nyberg P, Xie L, Kalluri R. Cancer Res 2005;65(10):3967–3979. [PubMed: 15899784]
4. Calzada MJ, Zhou L, Sipes JM, Zhang J, Krutzsch HC, Iruela-Arispe ML, Annis DS, Mosher DF, Roberts DD. Circ Res 2004;94(4):462–470. [PubMed: 14699013]
5. Chandrasekaran L, He CZ, Al-Barazi H, Krutzsch HC, Iruela-Arispe ML, Roberts DD. Mol Biol Cell 2000;11(9):2885–2900. [PubMed: 10982388]
6. Calzada MJ, Sipes JM, Krutzsch HC, Yurchenco PD, Annis DS, Mosher DF, Roberts DD. J Biol Chem 2003;278(42):40679–40687. [PubMed: 12909644]
7. Kerkhoff C, Sorg C, Tandon NN, Nacken W. Biochemistry 2001;40(1):241–248. [PubMed: 11141076]
8. McCormick CJ, Craig A, Roberts D, Newbold CI, Berendt AR. J Clin Invest 1997;100(10):2521–2529. [PubMed: 9366566]
9. Asch AS, Silbiger S, Heimer E, Nachman RL. Biochem Biophys Res Commun 1992;182(3):1208–1217. [PubMed: 1371676]
10. Dawson DW, Pearce SF, Zhong R, Silverstein RL, Frazier WA, Bouck NP. J Cell Biol 1997;138(3):707–717. [PubMed: 9245797]
11. Dawson DW, Volpert OV, Pearce SF, Schneider AJ, Silverstein RL, Henkin J, Bouck NP. Mol Pharmacol 1999;55(2):332–338. [PubMed: 9927626]
12. Jimenez B, Volpert OV, Crawford SE, Febbraio M, Silverstein RL, Bouck N. Nat Med 2000;6(1):41–48. [PubMed: 10613822]
13. Jimenez B, Volpert OV, Reiher F, Chang L, Munoz A, Karin M, Bouck N. Oncogene 2001;20(26):3443–3448. [PubMed: 11423995]
14. Huang MM, Bolen JB, Barnwell JW, Shattil SJ, Brugge JS. Proc Natl Acad Sci U S A 1991;88(17):7844–7848. [PubMed: 1715582]
15. Bull HA, Brickell PM, Dowd PM. FEBS Lett 1994;351(1):41–44. [PubMed: 7521304]
16. Thorne RF, Law EG, Elith CA, Ralston KJ, Bates RC, Burns GF. Biochem Biophys Res Commun 2006;351(1):51–56. [PubMed: 17052693]
17. Isenberg JS, Ridnour LA, Perruccio EM, Espey MG, Wink DA, Roberts DD. Proc Natl Acad Sci U S A 2005;102(37):13141–13146. [PubMed: 16150726]
18. Ignarro LJ. Curr Top Med Chem 2005;5(7):595. [PubMed: 16101421]
19. Milkiewicz M, Hudlicka O, Brown MD, Silgram H. Am J Physiol Heart Circ Physiol 2005;289(1):H336–H343. [PubMed: 15734877]
20. Yu J, deMuinck ED, Zhuang Z, Drinane M, Kauser K, Rubanyi GM, Qian HS, Murata T, Escalante B, Sessa WC. Proc Natl Acad Sci U S A 2005;102(31):10999–11004. [PubMed: 16043715]
21. Isenberg JS, Wink DA, Roberts DD. Cardiovasc Res 2006;71(4):785–793. [PubMed: 16820142]
22. Isenberg JS, Ridnour LA, Dimitry J, Frazier WA, Wink DA, Roberts DD. J Biol Chem 2006;281(36):26069–26080. [PubMed: 16835222]
23. Haviv F, Bradley MF, Kalvin DM, Schneider AJ, Davidson DJ, Majest SM, McKay LM, Haskell CJ, Bell RL, Nguyen B, Marsh KC, Surber BW, Uchic JT, Ferrero J, Wang YC, Leal J, Record RD, Hodde J, Badylak SF, Lesniewski RR, Henkin J. J Med Chem 2005;48(8):2838–2846. [PubMed: 15828822]

24. Hoekstra R, de Vos FY, Eskens FA, Gietema JA, van der Gaast A, Groen HJ, Knight RA, Carr RA, Humerickhouse RA, Verweij J, de Vries EG. J Clin Oncol 2005;23(22):5188–5197. [PubMed: 16051960]
25. Febbraio M, Hajjar DP, Silverstein RL. J Clin Invest 2001;108(6):785–791. [PubMed: 11560944]
26. Zhu W, Smart EJ. J Biol Chem 2005;280(33):29543–29550. [PubMed: 15970594]
27. Roberts DD, Cashel J, Guo N. J Tissue Cult Methods 1994;16:217–222.
28. Akiyama SK, Yamada KM. J Biol Chem 1985;260(7):4492–4500. [PubMed: 3920218]
29. Vogel T, Werber MM, Guy R, Levanon A, Nimrod A, Legrand C, Gorecki M, Eldor A, Panet A. Arch Biochem Biophys 1993;300(1):501–509. [PubMed: 8424687]
30. Harmon CM, Luce P, Beth AH, Abumrad NA. J Membr Biol 1991;121(3):261–268. [PubMed: 1865490]
31. Abumrad NA, el-Maghrabi MR, Amri EZ, Lopez E, Grimaldi PA. J Biol Chem 1993;268(24):17665–17668. [PubMed: 7688729]
32. Febbraio M, Abumrad NA, Hajjar DP, Sharma K, Cheng W, Pearce SF, Silverstein RL. J Biol Chem 1999;274(27):19055–19062. [PubMed: 10383407]
33. Bastie CC, Nahle Z, McLoughlin T, Esser K, Zhang W, Unterman T, Abumrad NA. J Biol Chem 2005;280(14):14222–14229. [PubMed: 15691844]
34. Koonen DP, Glatz JF, Bonen A, Luiken JJ. Biochim Biophys Acta 2005;1736(3):163–180. [PubMed: 16198626]
35. Maurer-Stroh S, Eisenhaber B, Eisenhaber F. J Mol Biol 2002;317(4):541–557. [PubMed: 11955008]
36. Liang X, Lu Y, Wilkes M, Neubert TA, Resh MD. J Biol Chem 2004;279(9):8133–8139. [PubMed: 14660555]
37. Waltenberger J, Claesson-Welsh L, Siegbahn A, Shibuya M, Heldin CH. J Biol Chem 1994;269(43):26988–26995. [PubMed: 7929439]
38. Lamalice L, Houle F, Huot J. J Biol Chem 2006;281(45):34009–34020. [PubMed: 16966330]
39. Busconi L, Michel T. J Biol Chem 1993;268(12):8410–8413. [PubMed: 7682550]
40. Liu J, Sessa WC. J Biol Chem 1994;269(16):11691–11694. [PubMed: 7512951]
41. Liu J, Garcia-Cardena G, Sessa WC. Biochemistry 1995;34(38):12333–12340. [PubMed: 7547976]
42. Murad F. Biosci Rep 2004;24(4–5):452–474. [PubMed: 16134022]
43. Lawler J, Weinstein R, Hynes RO. J Cell Biol 1988;107(6 Pt 1):2351–2361. [PubMed: 2848850]
44. Calzada MJ, Annis DS, Zeng B, Marcinkiewicz C, Banas B, Lawler J, Mosher DF, Roberts DD. J Biol Chem 2004;279(40):41734–41743. [PubMed: 15292271]
45. Iruela-Arispe ML, Lombardo M, Krutzsch HC, Lawler J, Roberts DD. Circulation 1999;100(13):1423–1431. [PubMed: 10500044]
46. Rioux V, Galat A, Jan G, Vinci F, D'Andrea S, Legrand P. J Nutr Biochem 2002;13(2):66–74. [PubMed: 11834221]
47. Eliceiri BP, Paul R, Schwartzberg PL, Hood JD, Leng J, Cheresh DA. Mol Cell 1999;4(6):915–924. [PubMed: 10635317]
48. Werdich XQ, Penn JS. Angiogenesis 2005;8(4):315–326. [PubMed: 16400523]
49. Tsuda S, Ohtsuru A, Yamashita S, Kanetake H, Kanda S. Biochem Biophys Res Commun 2002;290(4):1354–1360. [PubMed: 11812013]
50. Kanda S, Mochizuki Y, Nakamura T, Miyata Y, Matsuyama T, Kanetake H. J Cell Sci 2005;118(Pt 5):961–970. [PubMed: 15713745]
51. van't Hof W, Resh MD. J Cell Biol 1997;136(5):1023–1035. [PubMed: 9060467]
52. Koegl M, Zlatkine P, Ley SC, Courtneidge SA, Magee AI. Biochem J 1994;303(Pt 3):749–753. [PubMed: 7980442]
53. Vaandrager AB, Ehlert EM, Jarchau T, Lohmann SM, de Jonge HR. J Biol Chem 1996;271(12):7025–7029. [PubMed: 8636133]
54. Sessa WC, Barber CM, Lynch KR. Circ Res 1993;72(4):921–924. [PubMed: 7680289]
55. Kou R, Greif D, Michel T. J Biol Chem 2002;277(33):29669–29673. [PubMed: 12050171]
56. Perrino BA, Martin BA. J Biochem (Tokyo) 2001;129(5):835–841. [PubMed: 11328609]

57. Krotova K, Hu H, Xia SL, Belayev L, Patel JM, Block ER, Zharikov S. Br J Pharmacol 2006;148(5): 732–740. [PubMed: 16715118]
58. Sato Y. Biol Pharm Bull 2004;27(6):772–776. [PubMed: 15187415]
59. Kallander LS, Lu Q, Chen W, Tomaszek T, Yang G, Tew D, Meek TD, Hofmann GA, Schulz-Pritchard CK, Smith WW, Janson CA, Ryan MD, Zhang GF, Johanson KO, Kirkpatrick RB, Ho TF, Fisher PW, Mattern MR, Johnson RK, Hansbury MJ, Winkler JD, Ward KW, Veber DF, Thompson SK. J Med Chem 2005;48(18):5644–5647. [PubMed: 16134930]
60. Shintani S, Li C, Mihara M, Klosek SK, Terakado N, Hino S, Hamakawa H. Oral Oncol 2006;42(1): 66–72. [PubMed: 16140034]
61. Murata R, Nishimura Y, Hiraoka M. Int J Radiat Oncol Biol Phys 1997;37(5):1107–1113. [PubMed: 9169820]
62. Rofstad EK, Galappathi K, Mathiesen B. Int J Radiat Oncol Biol Phys 2004;58(2):493–499. [PubMed: 14751520]
63. Teicher BA, Holden SA, Ara G, Sotomayor EA, Huang ZD, Chen YN, Brem H. Int J Cancer 1994;57 (6):920–925. [PubMed: 7515861]
64. Yap R, Veliceasa D, Emmenegger U, Kerbel RS, McKay LM, Henkin J, Volpert OV. Clin Cancer Res 2005;11(18):6678–6685. [PubMed: 16166447]
65. French KJ, Zhuang Y, Schrecengost RS, Copper JE, Xia Z, Smith CD. J Pharmacol Exp Ther 2004;309 (1):340–347. [PubMed: 14724220]
66. Selvakumar P, Lakshmikuttyamma A, Dimmock JR, Sharma RK. Biochim Biophys Acta 2006;1765 (2):148–154. [PubMed: 16386852]

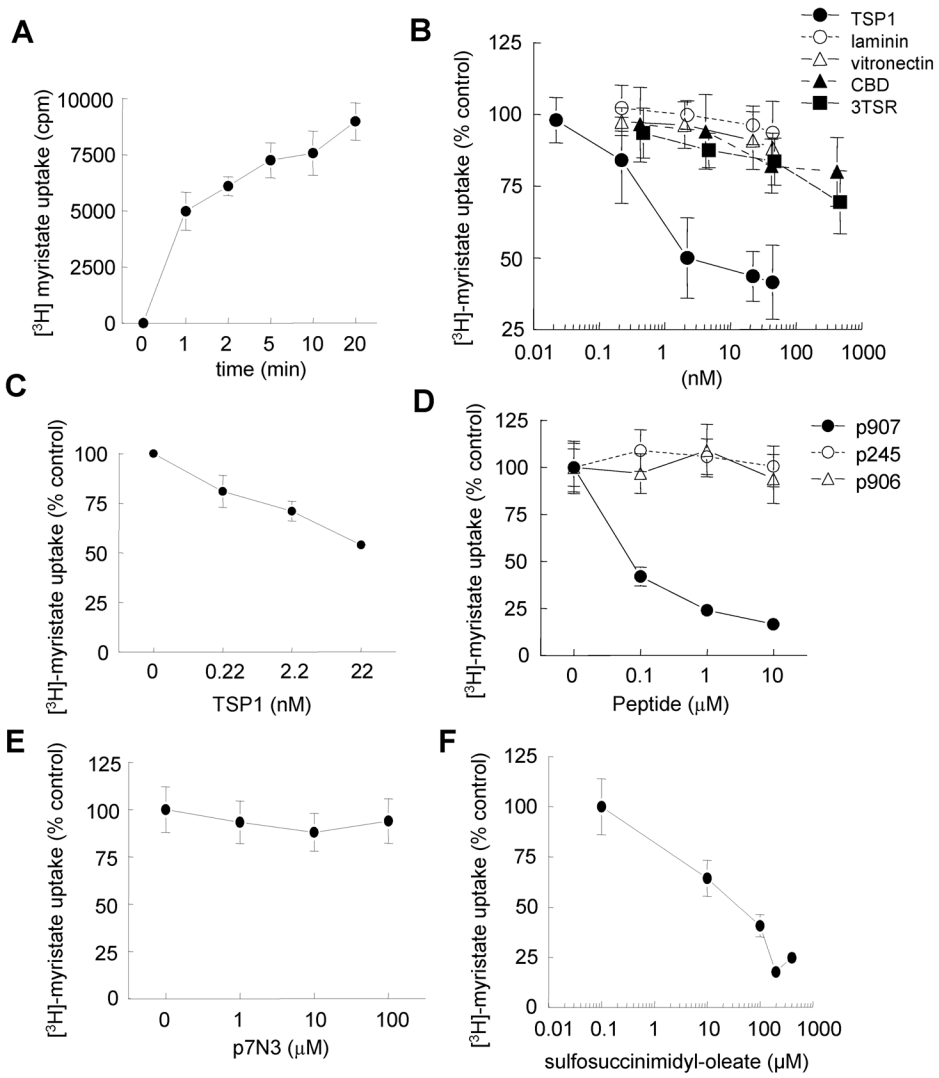

Fig. 1. Myristic acid uptake into vascular cells is inhibited by exogenous TSP1 and some CD36 binding peptides

A, D–F HUVEC or ***C***, HAVSMC (5×10^4 cells/well) were plated in 24-well culture plates in EGM + 2% FCS or SM-GM + 2% FCS respectively and weaned over 48 h to EBM or SM-BM + 0.1% FAF-BSA. ***A***, Cells were then treated with [^{3}H]-myristic acid complexed to FAF-BSA for the indicated time intervals, and uptake into cells was determined following lysis by scintillation counting. ***B***, [^{3}H]-Myristic acid uptake after 5 min into HUVEC was determined in the presence of the indicated concentrations of TSP1, its type 1 repeats (3TSR), its C-terminal domain (CBD), laminin or vitronectin. ***C***, Myristic acid uptake after 5 min into HAVSMC was determined in the presence of TSP1 (0.22 – 22 nM). ***D–F***, Uptake into HUVEC after 5 min was determined in the presence of CD36 binding peptides p907, p245 and p906 (0.1 – 10 μM, ***D***), the CD47 binding peptide p7N3 (1 – 100 μM, ***E***), or the CD36-specific translocase inhibitor sulfosuccinimidyl oleate (***F***).

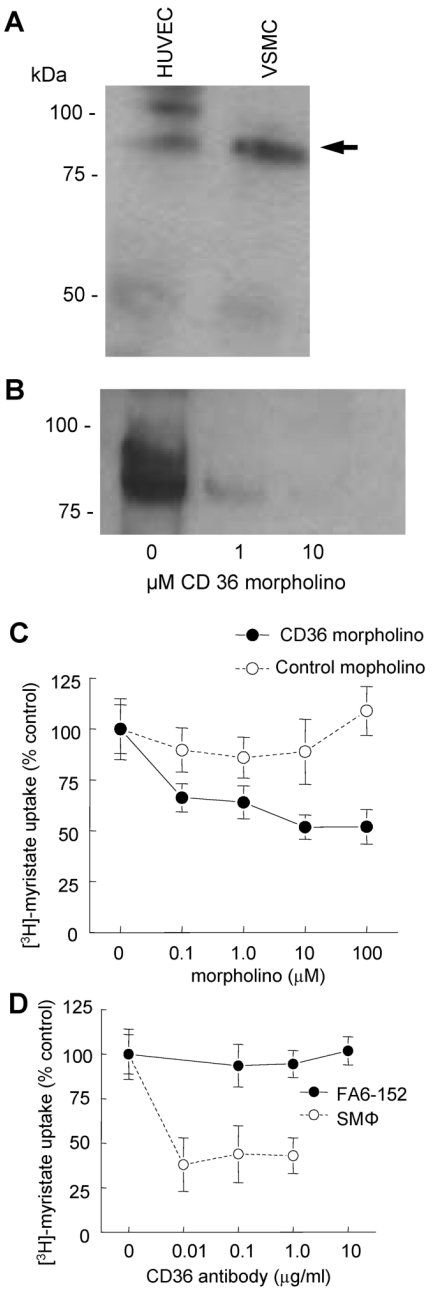

Fig. 2. Morpholino suppression of CD36 and a CD36 blocking antibody decrease myristate uptake into vascular cells

A, HUVEC and human aortic VSMC were cultured in standard growth medium, surface labeled with biotin, lysed, and immunoprecipitated using a monoclonal antibody to CD36. Equal amounts of protein were electrophoresed, transferred to membranes, and detected using strepavidin-peroxidase and chemiluminescent detection. ***B***, HAVSMC grown under standard growth conditions and treated for 48 with a CD36 morpholino (0 – 10 μM) and CD36 expression determined. ***C***, HUVEC (5×10^4 cells/well) were plated in 24-well culture plates in EGM + 2% FCS, treated with an antisense CD36 or control morpholino and weaned over 48 h to EBM + 0.1% BSA. Cells were then treated with [^{3}H]-myristic acid complexed to FAF-

BSA for 5 min., and uptake into cells was determined. ***D***, HUVEC were plated in 24-well culture plates in EGM + 2% FCS and weaned over 48 h to EBM + 0.1% FAF-BSA. Cells were then treated an agonist CD36 monoclonal antibody clone SMΦ or antagonist antibody clone FA6-152 at the indicated concentrations, incubated with [^{3}H]-myristic acid complexed to FAF-BSA for 5 min., and uptake into cells was determined as described.

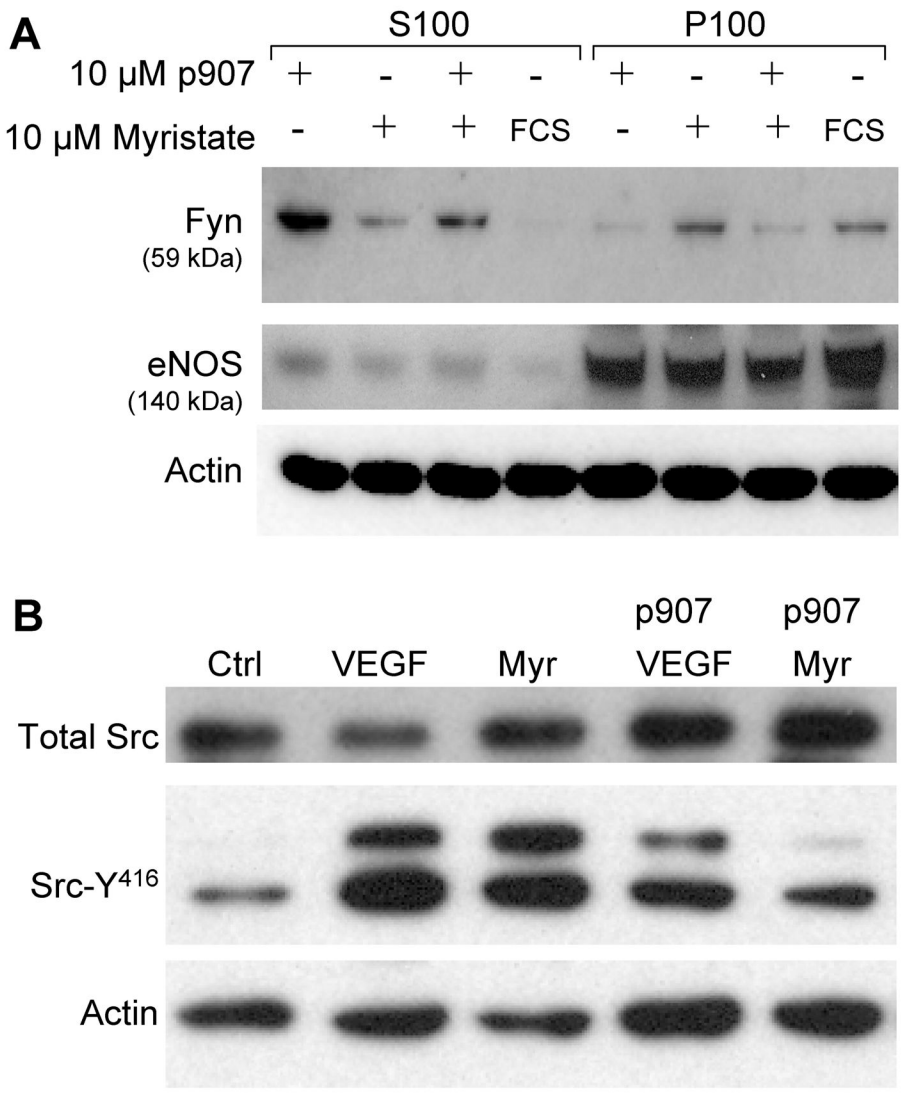

Fig. 3. Inhibition of CD36-mediated myristic acid uptake into endothelial cells by a TSP1-based peptide blocks rapid membrane translocation of Fyn and activation of Src kinases

A, HUVEC were plated into 100 mm plates and cultured in 2% FCS EGM to 80% confluence and serum starved over 24 h. The next day, cells were treated in EBM containing 0.1% FAF-BSA with or without peptide-907 (10 μM) for 15 min, ± myristate (10 μM) or EBM-1% FCS for 60 min. Cells were lysed, and the homogenate was separated by ultracentrifugation into membrane (P100) and cytosol fractions (S100). Proteins were separated by electrophoresis and analyzed by western blotting using Fyn and actin antibodies. ***B***, HUVEC were starved overnight in 1% FBS-EBM, rinsed and treated with the indicated reagents in EBM with 0.1% FAF-BSA: p907 at 10 μM for 15 min before the addition of VEGF or Myr. VEGF was added at 20 ng/ml for 5 min and myristate at 10 μM for 15 min. Cells were then rinsed with PBS and collected in SDS sample buffer. Westerns blots were probed with anti-Src-Y^{416} (Cell Signaling) or anti-Src (Cell Signaling). Membranes were reprobed with anti-actin antibody for loading control. Results presented are representative of three independent experiments.

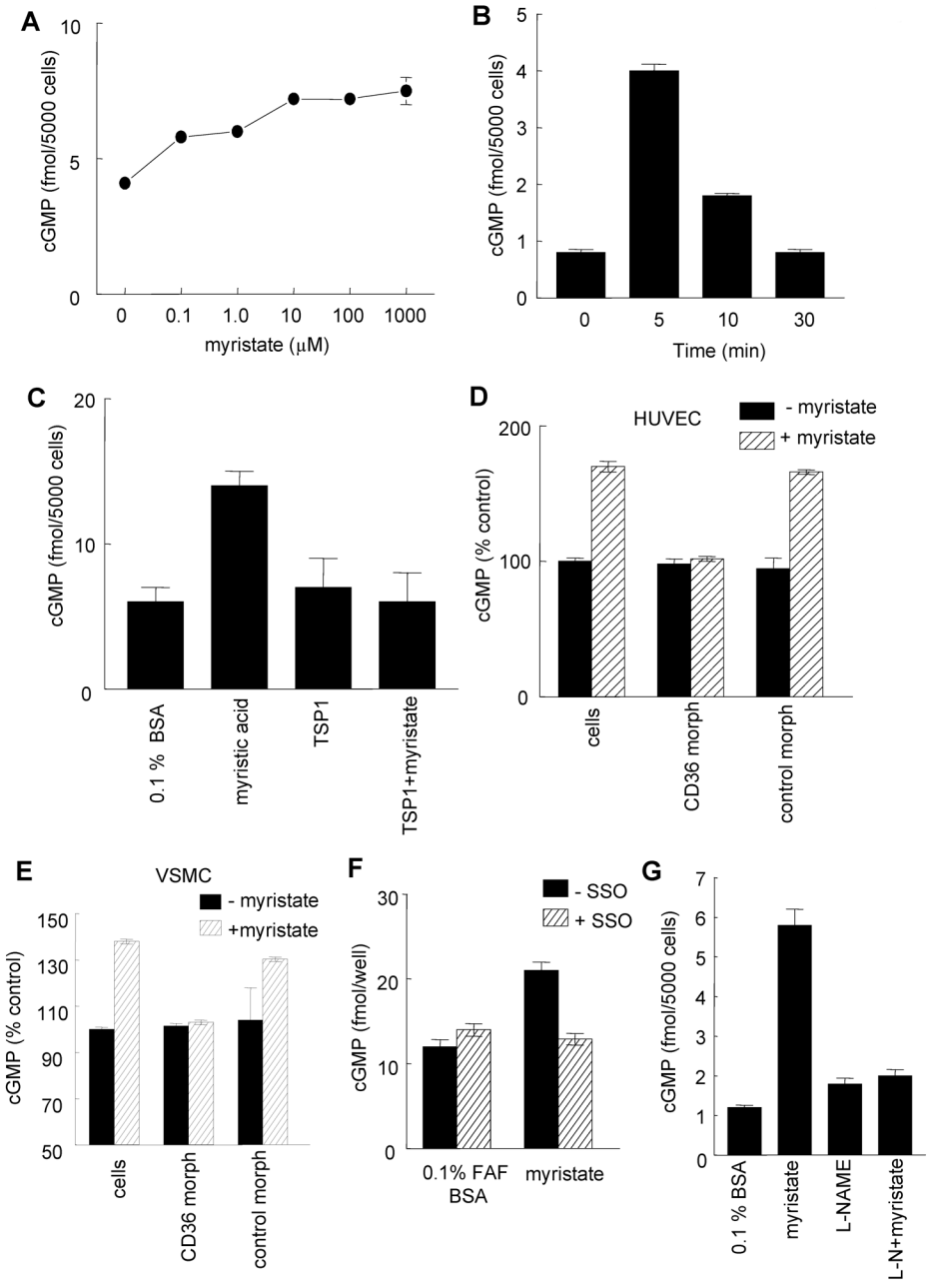

Fig. 4. TSP1 prevents myristic acid-stimulated cGMP accumulation in vascular cells mediated by CD36 and NOS

A–B, HUVEC plated at 5×10^3 cells/well were weaned over 48 h from serum and then treated in EBM containing 0.1% FAF-BSA with 0.1 – 100 μM myristic acid for 5 min (***A***), or with 10 μM myristic acid for the indicated times (***B***). Cells were lysed and cGMP levels determined via ELISA. ***C,D,F,G,*** Endothelial cells were pretreated with TSP1 for 15 min (1 μg/ml, ***C***), an antisense CD36 or control morpholino (10 μM ***D***) for 48 hours, SSO for 15 min (***F***), or L-NAME (500 μM, ***G***) and then with 10 μM myristate/FAF-BSA for 5 min. ***E***, HAVSMC were treated with an antisense CD36 or control morpholino (10 μM ***D***) for 48 hours and then with

10 μM myristate/FAF-BSA for 5 min. Cells were then lysed and cGMP levels determined. Results are representative of those obtained in three independent experiments.

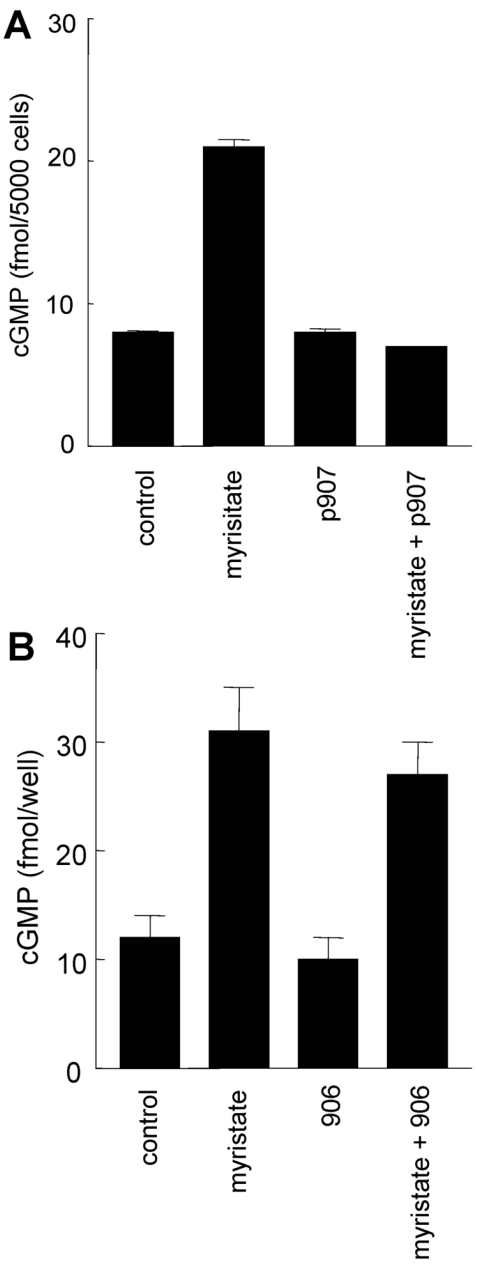

Fig. 5. A CD36-binding peptide prevents myristate-driven cGMP accumulation in endothelial cells

HUVEC cells plated at 5×10^3 cells/well were weaned over 48 h from serum then treated in EBM containing 0.1% FAF-BSA and pre-treated with the translocase inhibiting CD36-binding peptide (p907, ***A***) or control (p906, ***B***) (10 μM) for 15 min, treated with myristate (10 μM) for 5 min, and cGMP levels determined via ELISA.

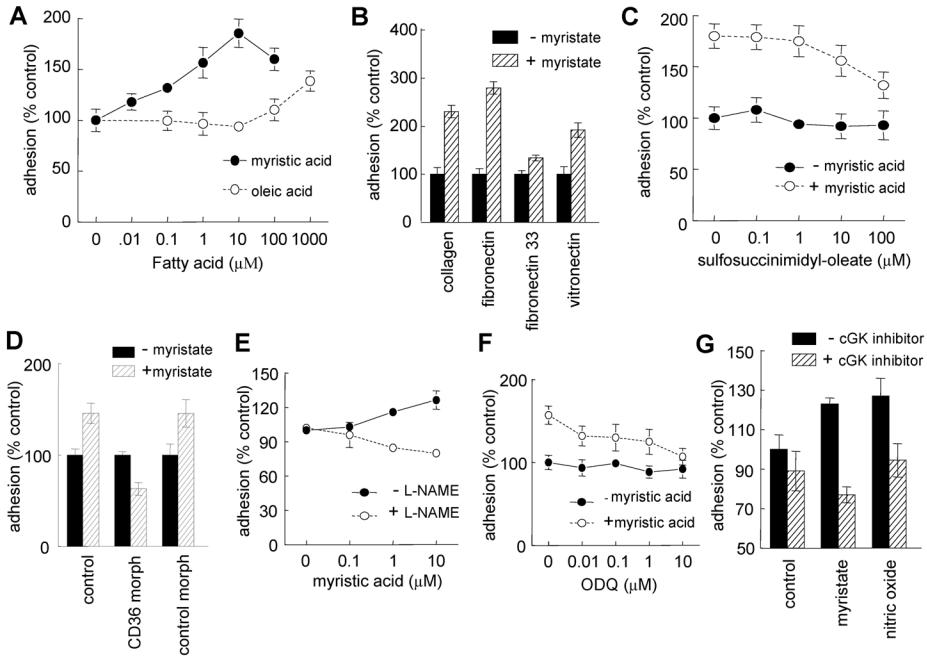

Fig. 6. Myristic acid stimulates endothelial cell adhesion to type I collagen via CD36/NOS/sGC/cGK signaling

HUVEC (10^4 cells/well) were plated in 96-well plates pre-coated with type I collagen (3 μg/ml) in EBM+0.1% FAF-BSA and the indicated concentrations of (***A***) myristic acid or oleic acid, (***C***) SSO ± myristic acid (10 μM), (***D***) cells pretreated for 48 h with an antisense CD36 or mismatched control morpholino (10 μM) ± myristic acid (10 μM), (***E***) myristic acid ± the NOS inhibitor L-NAME (500 μM), (***F***) the soluble guanylyl cyclase inhibitor ODQ (0.01 – 10 μM) ± myristic acid (10 μM), or (***G***) the cGK inhibitor Rp-8-*p*CPT-cGMPs (10 μM) ± myristic acid (10 μM) or DEA/NO (10 μM) and incubated for 1 h at 37° C and 5% CO_2. (***B***) HUVEC (10^4 cell/well) were plated in 96-well plates pre-coated with type I collagen (3 μg/ml), vitronectin (2 μg/ml), fibronectin (3 μg/ml), or FN-33 (3 μg/ml) in EBM + 0.1% FAF-BSA ± myristic acid (10 μM). Adherent cells were quantified after staining with crystal violet at 570 nm. Results are expressed as the mean ± SD of triplicates and are representative of at least three experiments.

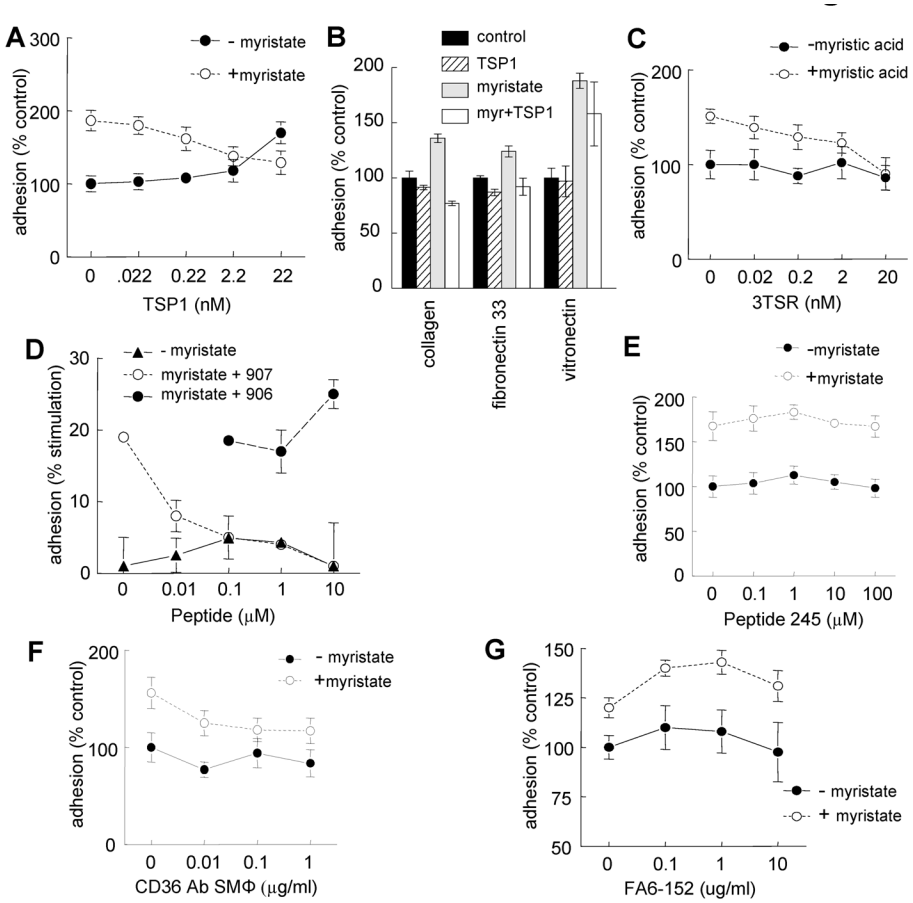

Fig. 7. CD36 ligands that inhibit fatty acid translocation prevent myristate-stimulated cell adhesion

HUVEC (10^4 cell/well) were plated in 96-well plates pre-coated with type I collagen (3 μg/ml) in EBM + 0.1% FAF-BSA ± myristic acid (10 μM) and the indicated concentrations of (***A***) TSP1, (***C***) 3TSR, (***D***) CD36-binding peptide 907 and control peptide 906, (***E***) noninhibitory CD36-binding peptide 245, (***F***) the uptake-blocking CD36 antibody SMΦ, or (***G***) the nonblocking CD36 antibody FA6-152 and incubated for 1 h at 37° C and 5% CO_2. (***B***) HAVSMC (10^4 cell/well) were plated in 96-well plates pre-coated with type I collagen (3 μg/ml), vitronectin (1 μg/ml), or FN-33 (1.5 μg/ml) in SM-BM + 0.1% FAF-BSA ± myristic acid (10 μM) ± TSP1 (2.2 nM). Adhesion was quantified by colorimetric assay at 570 nm. Results are expressed as the mean ± SD of triplicates and are representative of at least three experiments.

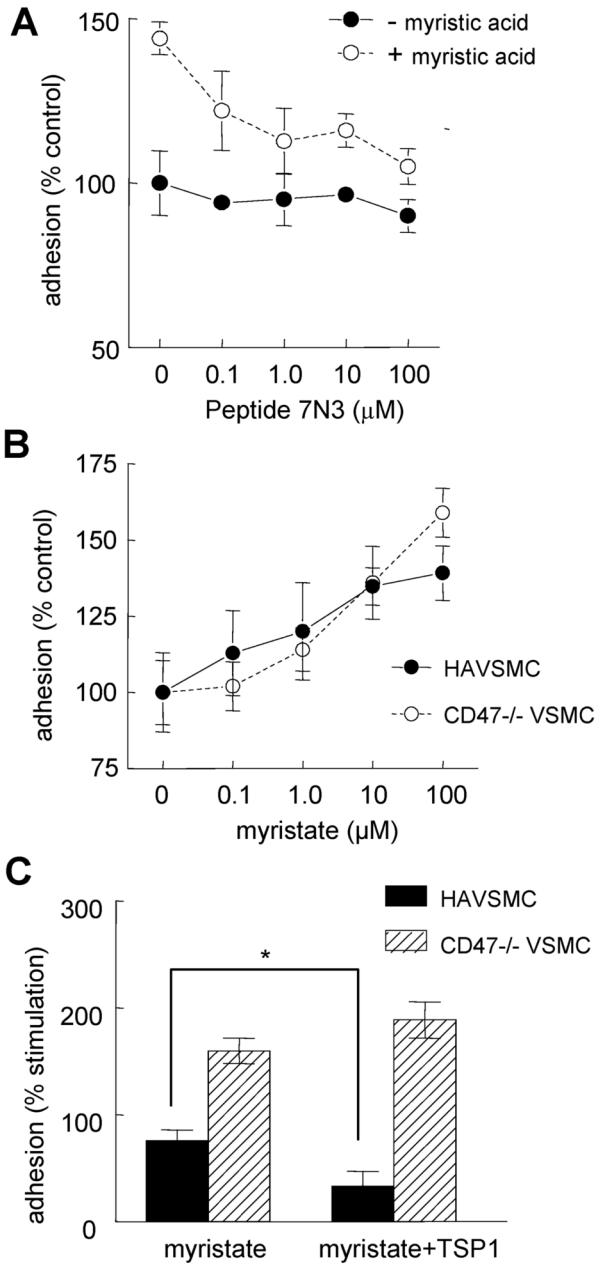

Fig. 8. CD47 is not necessary for stimulation of adhesion by myristate but is required for inhibition of this response by low concentrations of TSP1

HUVEC (10^4 cell/well) were plated in 96-well plates pre-coated with type I collagen (3 μg/ml) in EBM + 0.1% FAF-BSA and the indicated concentrations of (***A***) the CD47-binding peptide p7N3 (0.1 – 100 μM) ± myristic acid (10 μM) and incubated for 1 h at 37° C and 5% CO_2. Adhesion was quantified by colorimetric assay at 570 nm. (***B***), HAVSMC and CD47 null VSMC (10^4 cell/well) were plated in 96-well plates pre-coated with type I collagen (3 μg/ml) in SM-BM + 0.1% FAF-BSA and the indicated concentrations of myristic acid, or (***C***) myristic acid (10 μM) ± TSP1 (2.2 nM) and adhesion determined by colorimetric assay at 570 nm.

Results are expressed as the mean ± SD of triplicates and representative of at least three experiments.

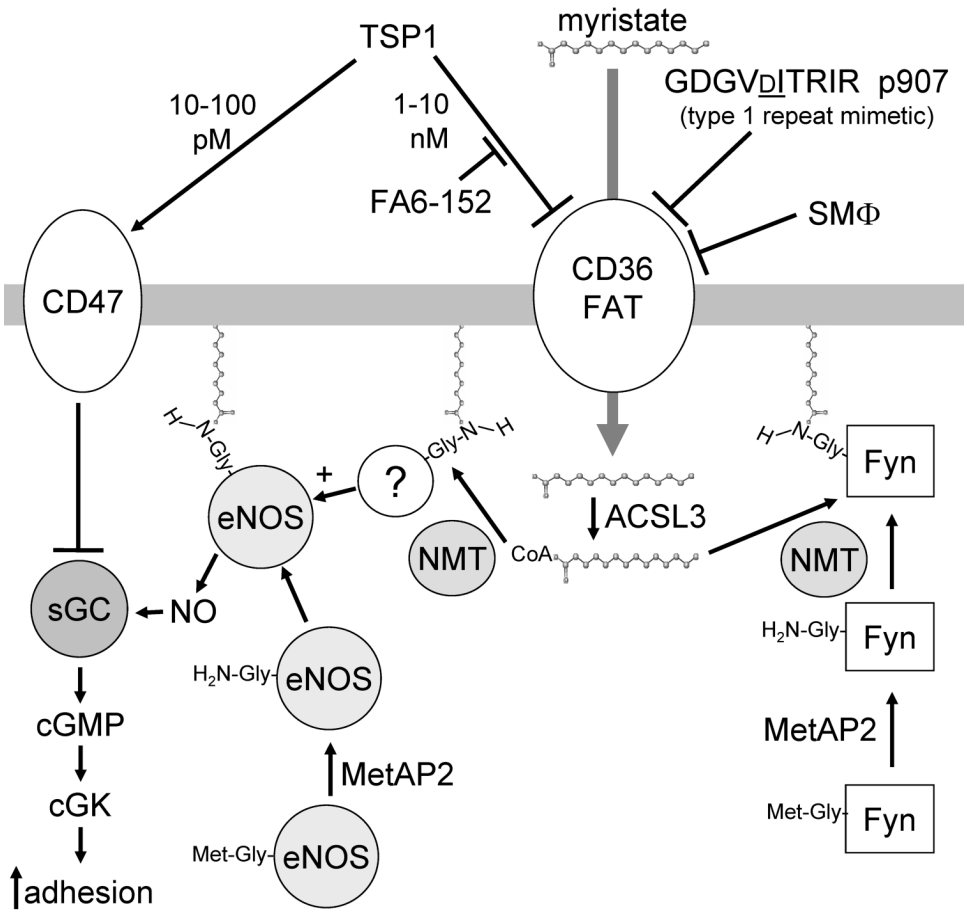

Fig. 9. Model for CD36-dependent activities of TSP1 and other CD36 ligands

Uptake of myristic acid via the fatty acid translocase (FAT) activity of CD36 is potently inhibited by the TSP1-derived mimetic p907 and by the angiogenesis-inhibiting CD36 antibody SMΦ (10). TSP1 inhibits FAT activity, and CD36 antibody FA6-152 is known to antagonize the anti-angiogenic activity of TSP1 (10,12,13) but does not itself inhibit FAT. In serum starved endothelial cells, inhibiting myristic acid transport is proposed to limit precursor for synthesis of myristoyl-CoA via the acyl-CoA synthase (ACSL3), which is then transferred by N-myristoyl transferases (NMT) to proteins bearing subterminal Gly residues exposed by Met aminopeptidases (MetAP). Of these, MetAP2 is the known target of several angiogenesis inhibitors (58), suggesting convergence of the signaling pathways induced by these inhibitors and TSP1. Limiting myristoylation prevents translocation of Fyn and other myristoylated proteins to membranes and indirectly limits eNOS activity. TSP1 at 1–10 nM limits cGMP signaling by inhibiting myristate uptake via CD36 and at 10–100 pM also inhibits sGC activation via CD47 (22).